Dynamics of vortex-antivortex matter in nanostructured ferromagnet-superconductor bilayers

Cléssio L. S. Lima[1,2] and Clécio C. de Souza Silva[1]
[1]*Departamento de Física, Universidade Federal de Pernambuco, 50670-901 Recife, PE, Brazil*
[2]*Instituto de Física, Universidade Federal do Rio de Janeiro, CP 68528, 21945-970 Rio de Janeiro, RJ, Brazil*
(Received 11 July 2008; revised manuscript received 17 July 2009; published 21 August 2009)

We investigate theoretically the dynamics of vortices and antivortices in a hybrid superconductor magnetic-dot-array bilayer with the nanodots polarized in plane. Our model naturally accounts for creation and annihilation of vortex-antivortex (v-av) pairs and simulate their motion by a (Langevin) molecular-dynamics algorithm. We observed several phenomena resulting from the intricate vortex-antivortex dynamics in this system. In general, as a dc-transport current is applied, the steady state corresponds to a cyclic sequence of vortex-antivortex creation, motion and annihilation processes, giving rise to periodic fluctuations of the number of v-av pairs and the induced electric field. Surprisingly, the v-av motion does not follow, in general, the induced Lorentz force direction. Hence, a vortex-guidance effect and the resulting transverse electrical field were observed at zero external magnetic field when the current was applied near certain high-symmetry directions.

DOI: 10.1103/PhysRevB.80.054514 PACS number(s): 74.25.Qt, 74.78.Na

I. INTRODUCTION

Technological applications of superconductors are strongly influenced by magnetic-flux quanta (vortices) present in all type-II superconducting materials. The current-carrying capabilities of superconductors are determined by the ability of certain inhomogeneities inside the material to pin vortices down, preventing their dissipative motion. In superconducting films, nanoengineered arrays of pinning centers, such as antidots,[1] blindholes,[2,3] magnetic,[4–9] and nonmagnetic dots,[5,10] have been demonstrated to provide very efficient mesoscopic trapping of vortices. As a result, the maximum current supported by such nanostructured films can be orders of magnitude higher than those measured in the corresponding pristine film.

Among the variety of artificial pinning centers, magnetic dots arise as a specially interesting option in part because of the tunability of their magnetic moments and, consequently, of their flux-pinning properties. Indeed, as it has been experimentally demonstrated, nanomagnets can trap vortices, either by local reduction of the critical temperature via the proximity effect[4,5] or by their magnetic flux when the dots are polarized.[7,8,11] In the last case, the material is sensible to the specific polarization of the external magnetic field. Therefore, although ferromagnets usually inflicts a destructive effect on superconductors, conveniently nanostructured compositions such as those mentioned above are able to enhance the critical properties of superconducting films in a very controllable way.

Another interesting feature of these systems is that, for strong enough magnetic moments, magnetic dots have the unique ability of inducing spontaneous vortex-antivortex (v-av) pairs in the superconductor and keep them from annihilating each other even when thermal fluctuations are negligible.[12,13] This topic has attracted a great deal of attention lately. Several calculations using the Ginzburg-Landau approach have been carried out for arrays of polarized magnetic dots on top of a superconducting film predicting a great variety of equilibrium phases, including vortex-antivortex ionic molecules and composite vortex-antivortex lattices.[14–17]

The formation and implications of vortex-antivortex matter in hybrid superconductor-ferromagnet systems is currently a matter of intense debate. A few experimental works have provided indirect and even direct demonstrations of the formation of spontaneous v-av patterns and their implications. Transport measurements on superconducting films in the presence of off-plane magnetic-dot arrays have suggested that the enhancement of superconductivity by a finite external magnetic field, the so-called field-induced superconductivity effect, stems from the annihilation of spontaneous antivortices (formed in the interstitial positions) with vortices added in by the external field.[18,19] Measurements on superconducting films with arrays of in-plane magnetized microbars demonstrated a unique vortex-ratchet effect at zero applied magnetic field presumably resulting from the asymmetric motion of spontaneous vortices and antivortices.[20] More recently, scanning Hall-probe microscopy of superconducting films with arrays of magnetic dots of different sizes has provided a direct corroboration of some equilibrium vortex-antivortex patterns predicted theoretically.[21]

Despite the intense research on this subject, little is known about the actual microscopic dynamics of vortices and antivortices and how it gives rise to the great variety of transport phenomena macroscopically observed in experiments. Here we address this point by performing numerical simulations of vortices and antivortices in a hybrid superconductor magnetic-dot-array bilayer. Our calculations reveal the intricate dynamics of spontaneous vortex-antivortex pairs when a transport current is applied onto the bilayer at zero magnetic field and how it affects the bilayer electrical response. We also demonstrate a unique transverse voltage effect at zero magnetic field caused by average guided motion of vortices and antivortices.

II. MODEL AND SIMULATION DETAILS

The details of our model is as follows. The bilayer comprises a thin superconducting film of thickness d, penetration depth $\lambda \gg d$, and coherence length $\xi < d$. A square array of magnetic dipoles, with magnetic moment $\mathbf{m}$ and unit cell of

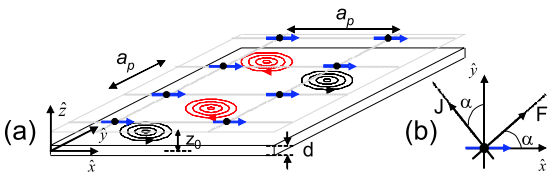

FIG. 1. (Color online) (a) Schematic view of the in-plane dipole array. (b) Definition of the transport current **J** and driving force **F** orientations.

dimensions $a_p \times a_p$ (Fig. 1), is placed above the film, at a distance $z_0 > d/2$ from it. Experimentally, the space between the superconducting film and the dipole layer is usually filled with an insulating buffer layer to prevent proximity effects. Here we assume that the dipoles are polarized in plane, parallel to the x direction ($\mathbf{m}=m\hat{\mathbf{x}}$). The total energy of the vortex matter is given by

$$E = \sum_{i,j} q_i q_j \left[\frac{1}{2} U_{\mathrm{vv}}(\mathbf{r}_{ij}) + E_c \delta_{i,j} \right] + \sum_j q_j U_{\mathrm{vm}}(\mathbf{r}_j), \qquad (1)$$

where q is the vorticity ($q=1$ for vortices, $q=-1$ for antivortices). Here we assume that no external magnetic field is applied. In other words, the vortex-matter "neutrality" condition, $\Sigma_j q_j = 0$, must be satisfied. $U_{\mathrm{vm}}(\mathbf{r})$ is the usual interaction energy between a vortex located at $\mathbf{r}$ and the dipole array calculated in the London limit.[22] The interaction energy $U_{\mathrm{vv}}(\mathbf{r}_{ij})$ between an arbitrary pair of vortices at positions $\mathbf{r}_i$ and $\mathbf{r}_j$ is calculated following Clem's variational approach for the order parameter ($\mathbf{r}_{ij}=\mathbf{r}_i-\mathbf{r}_j$).[23] In the limit $\lambda \gg d$ considered here, this gives $U_{\mathrm{vv}}(\mathbf{r}) = \varepsilon_0 d \ln(|\mathbf{r}_{ij}|^2 + 2\xi_c^2)$, where $\varepsilon_0 = \phi_0^2/4\pi\mu_0\lambda^2$ and ξ_c is a variational parameter [in general, $\xi_c \sim \xi(T)$]. The vortex-core energy can be calculated straightforwardly by using Clem's trial order parameter to compute the gain in condensation energy due to an isolated vortex, which results in $E_c = 0.375\varepsilon_0$. $-E_c$ acts as a chemical potential of the vortex system and thus plays an important role in the nucleation of vortex-antivortex pairs.[24]

Our numerical algorithm is based on the assumption that the time evolution of the vortex matter can be broken into two distinct parts: motion of the vortices and antivortices, and creation of v-av pairs. The first is governed by the Langevin equation

$$\eta \frac{d\mathbf{r}_j(t)}{dt} = -\nabla_j E + \mathbf{F}_j + \mathbf{\Gamma}_j, \qquad (2)$$

where $\eta = \mu_0 \phi_0 H_{c2}/\rho_n$ is the Bardeen-Stephen friction coefficient (with $H_{c2} = \phi_0/2\pi\xi^2$ and ρ_n the normal-state resistance), j runs over all vortices and antivortices present at time t, $\mathbf{F}_j = q_j \phi_0 \mathbf{J} \times \hat{\mathbf{z}}$ is the driving force, and $\mathbf{\Gamma}_j$ is the random force appropriate to temperature T. **J** is the applied current density which makes an angle α with the positive y axis, as shown in Fig. 1(b). These equations are solved numerically by a finite difference method. Eventually, a vortex and an antivortex collide and annihilate each other. This is taken into account by assuming that such a collision occurs every time the vortex and the antivortex are separated by a distance $\leq \xi_c$.

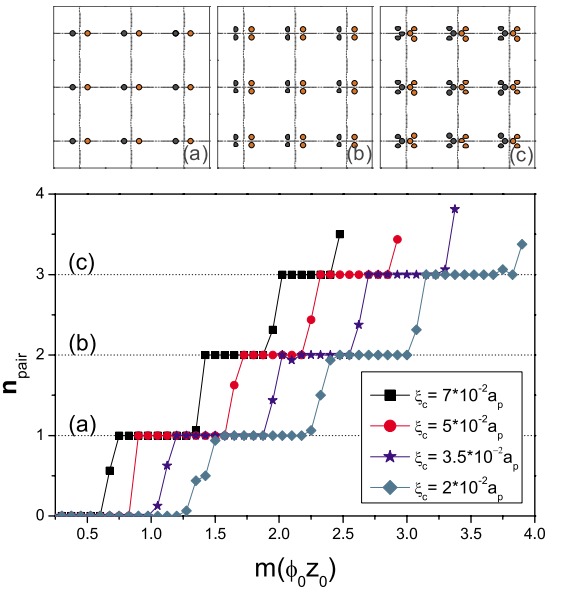

FIG. 2. (Color online) (Top) Vortex(black)-antivortex(red) configurations for (a) $m=1.0\phi_0 z_0$ ($n_{pair}=1$), (b) $m=1.65\phi_0 z_0$ ($n_{pair}=2$) and (c) $m=2.25\phi_0 z_0$ ($n_{pair}=3$). (Bottom) Number of v-av pairs per dipole, n_{pair}, versus magnetic moment of the dipoles, m, for different values of ξ_c.

The procedure for the second part, v-av pair creation, is to freeze the vortex-matter configuration after every Langevin dynamics time step and create v-av pairs using a Monte Carlo procedure. This assumes that the actual nucleation process takes place in a time interval so short that the motion of the vortex matter during it can be neglected.[16] Trial v-av pairs are then placed at every point of an auxiliary grid, with unit cell of dimensions $a_c \times a_c$ ($a_c \simeq \xi_c$), commensurate with the dipole array. The vortex and antivortex are placed at a distance ξ_c from each other at a given axis, with the pair center of mass fixed at the grid point. At high T, this axis is chosen randomly, whereas at low T it is determined by the direction of the total current density calculated at the grid point (at that instant of time) as to favor pair unbinding. Then, a Metropolis code is used to either accept or reject the pair. The energy entering this algorithm includes the energy due to the interaction with the transport current, that is $E_T = E - \Sigma_j \mathbf{F}_j \cdot \mathbf{r}_j$. Such a procedure accounts for both deterministic (induced by the local-current distribution) and thermal pair nucleation.[25]

III. EQUILIBRIUM CONFIGURATIONS

The simulations are carried out on a $L \times L$ section of the bilayer, with $L = 8a_p$, and assuming periodic boundary conditions in both x and y directions. The time step used in the numerical integration is $dt = 2 \times 10^{-4} t_0$ [$t_0 = \eta a_p^2/d\varepsilon_0$]and we chose $z_0 = 0.2a_p$. Equilibrium configurations of the vortex matter for small T and $\mathbf{J}=0$, were obtained minimizing E (Eq. (1)) by means of a simulated annealing scheme. Figure 2 shows the equilibrium states of the superconducting film obtained by this method. The bottom panel presents the number of vortex-antivortex pairs per dipole (n_{pair}) as a function

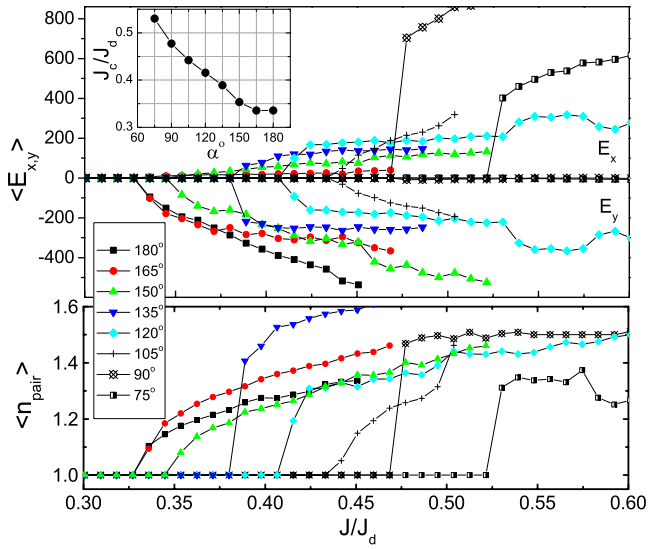

FIG. 3. (Color online) Time averages of the x and y components of the electric field (top) and of the v-av pair density (Bottom) as functions of the current density applied at different orientations α (measured with respect to the y axis). Inset: angular dependence of the critical current, $J_c(\alpha)$.

of the magnetic moment of the dipoles for several values of ξ_c. These curves are characterized by plateaus at integer n_{pair}. Examples of stable vortex-antivortex configurations for $\xi_c=7\times10^{-2}a_p$ are depicted in the upper panels. Notice that by increasing ξ_c (for instance, by increasing the temperature) the magnetic moment necessary for the creation of a new v-av pair per dipole decreases. This is consistent with the fact that the force necessary to separate a v-av pair decreases with ξ_c. Therefore, for lower ξ_c values, a strong magnetic moment is necessary to hold the pair from annihilating each other. A similar temperature dependence of the critical magnetic moment has also been observed in numerical calculation for magnetic-dot arrays in the off-plane geometry.[15,16]

IV. VORTICES AND ANTIVORTICES ON THE MOVE

Now we discuss the response of the vortex matter to an applied current flow. For simplicity, we shall consider hereafter only the cases where each dipole stabilizes one v-av pair in equilibrium, by assuming $\xi_c=7\times10^{-2}a_p$ and $m=1.0\phi_0 z_0$. Figure 3(a) presents the x and y components of the mean electric field induced by vortex motion, expressed by the time average of $\mathbf{E}=\phi_0\Sigma q_i\dot{\mathbf{r}}_i\times\hat{z}$, as a function of the current density $\mathbf{J}$ (in units of the depairing current J_d) for different orientations of $\mathbf{J}$. Averages were taken over 15×10^6 time steps after a relaxation waiting time of 5×10^6 time steps.

The $E_x(J)$ and $E_y(J)$ curves in Fig. 3(a) evidence a strong dependence of the v-av dynamics on the current orientation α. This anisotropy becomes clearer when one plots the critical current J_c as a function of α. Vortices are depinned more easily when $\mathbf{J}$ is at an angle $\alpha=180°$. At this direction, $\mathbf{J}=-J\hat{y}$ induces a Lorentz force on the vortices (antivortices)

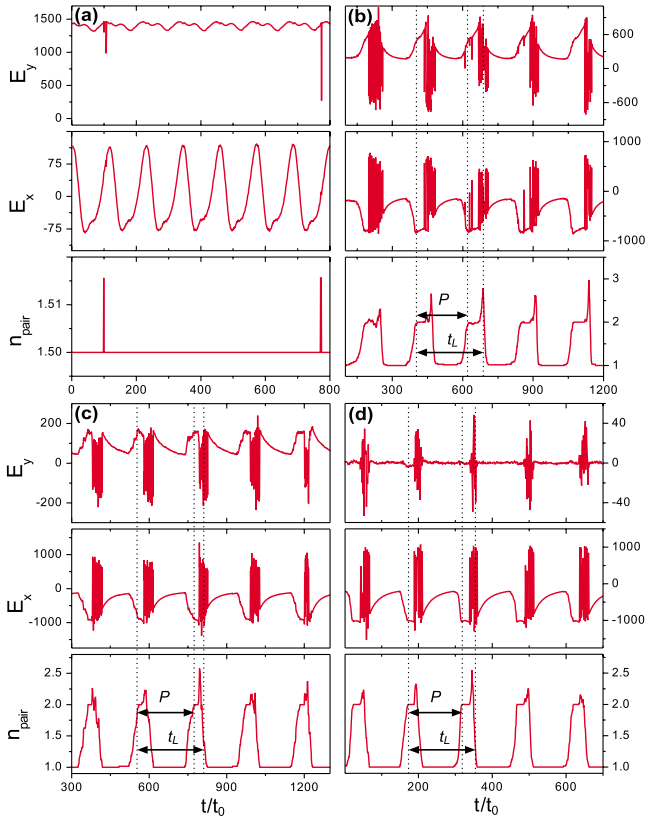

FIG. 4. (Color online) Time series of the electric field E_x, E_y, and v-av pair density n_{pair} for (a) $\alpha=90°$, (b) 120°, (c) 150°, and (d) 180°, and fixed current intensity $J=1.3J_c(\alpha)$.

parallel to $-\hat{x}$ $(+\hat{x})$ in such a way as to separate the v-av pairs. Such separation is favored by the supercurrent generated right below each dipole, which is also parallel to $-\hat{y}$ and is responsible for the stabilization of the v-av pairs. At $\alpha=90°$, on the other hand, the applied current has to overcome alone the v-av mutual attraction, with no help from the dipole-induced supercurrent. For $\alpha<90°$, the component J_y inverts sign and tends to bind the v-av pair. At $\alpha=75°$, J_x is still strong enough to unbind the pairs. At lower α, however, all v-av pairs annihilate each other and the current necessary to create new pairs and establish a dynamical state of moving v-av matter is close to J_d. At such current range, our model is no longer valid and therefore J_c could not be estimated for $\alpha<75°$. Figure 3(b) presents the mean v-av pair density $\langle n_{pair}\rangle$ as a function of $\mathbf{J}$. Interestingly, for all angles studied the onset of v-av matter motion is accompanied by an increase in $\langle n_{pair}\rangle$ with respect to the static (equilibrium) value $\langle n_{pair}\rangle=1$.

Here we analyze in more detail the dynamics of vortices and antivortices in the film and how it affects the macroscopic electrical response and the mean pair density. We shall restrict ourselves to four directions, $\alpha=180°$, $\alpha=150°$, $\alpha=120°$, and $\alpha=90°$. Figure 4 presents the time evolution of the number of v-av pairs per dipole and the x and y components of the mean electric field for fixed $\mathbf{J}$ values. For $J>J_c(\alpha)$, we observed steady states of the moving v-av matter characterized by an oscillatory time dependence of E_x and E_y, even though the applied current is constant. For $\alpha=90°$,

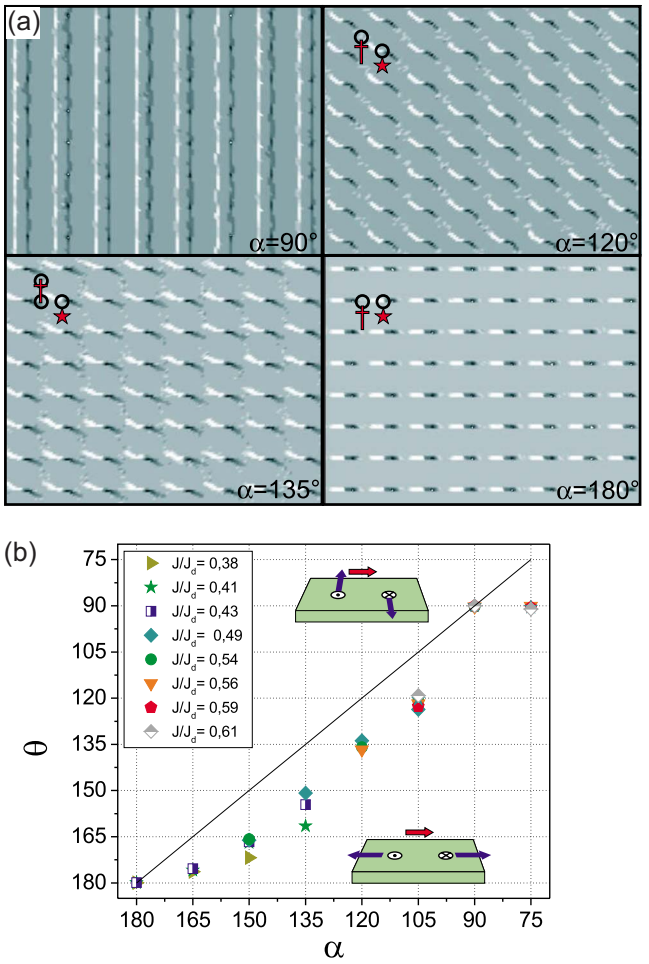

FIG. 5. (Color online) (a) Time-averaged vortex density for $J=0.5J_d$ and different current orientations α. Light (dark) shades correspond to vortices (antivortices). The circles indicate creation ($\star$) and annihilation (†) of v-av pairs. (b) Electric field direction θ as a function of α for several driving-current intensities (symbols). The $\theta=\alpha$ line is shown for comparison. The cartoons illustrate the dominating v-av motion for $\theta\sim 180°$ and $\theta\sim 90°$.

$n_{pair}(t)$ rapidly reaches 1.5 and keeps essentially constant at this value. The corresponding steady state is illustrated in Fig. 5(a), where we present contour plots of the time-averaged vortex-antivortex density, defined as $\rho(\mathbf{r})=\langle\Sigma_i q_i \delta[\mathbf{r}-\mathbf{r}_i(t)]\rangle_t$. The average is taken at a fixed $\mathbf{J}$ over N_S time steps. The trajectories of vortices (antivortices) are given by the light (dark) color shades. As it is clear, vortices and antivortices follow distinct tracks, perpendicular to the applied current, and collide very rarely.

For $\alpha>90°$, the dynamical steady states are much richer. Not only $\mathbf{E}(t)$ but also $n_{pair}(t)$ is oscillatory, indicating a cyclic series of creation and annihilation of v-av pairs. The general picture is as follows: when a current $J>J_c(\alpha)$ is applied, the vortices and antivortices stabilized by the dipoles in the equilibrium ($J=0$) state, which we shall refer to as first-generation vortices, depin and move apart from each other, leaving space for the creation of new (second-generation) v-av pairs right below the dipoles. At this point, $n_{pair}(t)$ reaches twice its original value [$n_{pair}(t)=2$]. These new pairs, give an additional push to the preexistent ones, inducing a sudden increase in $|\mathbf{E}|$. All first-generation vortices and antivortices run toward annihilation, which will take place at the midpoint between first-neighbor dipoles, for $135°\leq\alpha\leq 180°$, or at the face center of the dipole array unit cells, for $105°\leq\alpha<135°$, as revealed by the $\rho(\mathbf{r})$ plots presented in Fig. 5(a). Just before annihilation, however, new v-av pairs spawn at the above mentioned positions and subsequently annihilate the first-generation vortices and antivortices. We believe these extra (third-generation) pairs, which have a very short lifetime, arise from the fact that our model assumes a rigid vortex core. At distances of order ξ, the v-av annihilation in superconductors is characterized by strong vortex-core deformation. In our model, the extra v-av pairs appear naturally as a way of compensating the vortex-core rigidity and accelerate the annihilation process. As a side effect, a spurious, high-frequency noise arises in $E_x(t)$ and $E_y(t)$. Nevertheless, we have checked that such noise has only a negligible influence on the macroscopic quantities shown in Fig. 3. Finally, after the annihilation event, the second-generation v-av pairs become first-generation ones and the whole process repeats. Notice that the lifetime, t_L, of a vortex of the first or second generation is always larger than the oscillation period P (see Fig. 4).

The angular dependence of the v-av dynamics described above suggests that motion occurs preferentially along the x directions for α close to 180°. Such guided motion of the v-av matter should be reflected by the electric field $\mathbf{E}$ generated by vortex motion, giving rise to a deflection of $\mathbf{E}$ with respect to $\mathbf{J}$ and thus inducing transverse resistance. To demonstrate this statement, we plot the direction of $\mathbf{E}$, θ, as a function of the direction of $\mathbf{J}$, α, for several values of J (left panel of Fig. 5). Indeed, $\theta(\alpha)$ diverges considerably from the $\theta=\alpha$ line. For α close to 180°, θ tends to lock at $\theta\simeq 180°$ in the whole J range, whereas for $\alpha=75°$, $\mathbf{E}$ locks at $\theta=90°$. The transverse resistance resulting from the guided motion of v-av matter observed here is essentially different from that observed in superconducting films with nonmagnetic pinning arrays[26,27] and other Hall-type effects in the sense that here no macroscopic magnetic field is required.

V. CONCLUSIONS

In summary we have investigated by numerical simulations the dynamics of vortices and antivortices in superconducting films interacting with an array of in-plane magnetic dots. We developed a method for molecular-dynamics simulation of vortices and antivortices which accounts for their creation and mutual annihilation. Our calculations on the dynamics of current-driven vortices and antivortices revealed a periodic sequence of creation and annihilation of vortex-antivortex pairs. These events take place synchronously nearby every magnetic dot, giving rise to a sharp oscillatory behavior of the pair density and, consequently, of the electric field. Such ac response induced by a dc current can be cross-checked by time-resolved transport experiments. In addition, owing to the presence of vortices and antivortices at $H=0$ and their interaction with the dipole array, the critical current (J_c) at this field value is strongly anisotropic. Another important prediction of our model is the observation of a trans-

verse electric field induced by vortex-antivortex guidance. This is a unique Hall-type effect observed at *zero (macroscopic) magnetic field*. It is worth noticing that recently similar anisotropy in J_c as well as guided vortex motion has been observed experimentally in superconducting films interacting with different magnetic textures for the case of nonzero magnetic fields, as a result of the inherently anisotropic properties of the magnetic pinning potential.[9,28] The anisotropy and guidance observed in our calculations, on the other hand, occur at zero field and is only possible if the specific magnetic texture is capable of inducing spontaneous v-av pairs. In this sense, these phenomena, when observed at zero magnetic field, can be considered as fingerprints of spontaneous vortex-antivortex matter in superconductor-ferromagnetic hybrids.

ACKNOWLEDGMENTS

The authors are grateful to Gilson Carneiro for fruitful discussions. Research supported in part by the Brazilian agencies CNPq and CAPES.

[1] V. V. Moshchalkov, M. Baert, V. V. Metlushko, E. Rosseel, M. J. Van Bael, K. Temst, R. Jonckheere, and Y. Bruynseraede, Phys. Rev. B **54**, 7385 (1996); A. V. Silhanek, S. Raedts, M. Lange, and V. V. Moshchalkov, *ibid.* **67**, 064502 (2003).

[2] A. Bezryadin, Yu. N. Ovchinnikov, and B. Pannetier, Phys. Rev. B **53**, 8553 (1996).

[3] S. Raedts, A. V. Silhanek, M. J. Van Bael, and V. V. Moshchalkov, Phys. Rev. B **70**, 024509 (2004).

[4] J. I. Martin, M. Vélez, J. Nogués, and I. K. Schuller, Phys. Rev. Lett. **79**, 1929 (1997).

[5] Y. Jaccard, J. I. Martín, M.-C. Cyrille, M. Vélez, J. L. Vicent, and Ivan K., Schuller, Phys. Rev. B **58**, 8232 (1998); A. Hoffmann, P. Prieto, and I. K. Schuller, *ibid.* **61**, 6958 (2000).

[6] D. J. Morgan and J. B. Ketterson, Phys. Rev. Lett. **80**, 3614 (1998).

[7] M. J. Van Bael, K. Temst, V. V. Moshchalkov, and Y. Bruynseraede, Phys. Rev. B **59**, 14674 (1999).

[8] M. J. Van Bael, J. Bekaert, K. Temst, L. Van Look, V. V. Moshchalkov, Y. Bruynseraede, G. D. Howells, A. N. Grigorenko, S. J. Bending, and G. Borghs, Phys. Rev. Lett. **86**, 155 (2001) ; M. J. Van Bael, M. Lange, S. Raedts, V. V. Moshchalkov, A. N. Grigorenko, and S. J. Bending, Phys. Rev. B **68**, 014509 (2003).

[9] A. Belkin, V. Novosad, M. Iavarone, J. Pearson, and G. Karapetrov, Phys. Rev. B **77**, 180506(R) (2008); V. Vlasko-Vlasov, U. Welp, G. Karapetrov, V. Novosad, D. Rosenmann, M. Iavarone, A. Belkin, and W.-K. Kwok, *ibid.* **77**, 134518 (2008).

[10] G. Karapetrov, J. Fedor, M. Iavarone, D. Rosenmann, and W. K. Kwok, Phys. Rev. Lett. **95**, 167002 (2005).

[11] J. E. Villegas, K. D. Smith, L. Huang, Y. Zhu, R. Morales, and I. K. Schuller, Phys. Rev. B **77**, 134510 (2008).

[12] S. Erdin, A. F. Kayali, I. F. Lyuksyutov, and V. L. Pokrovsky, Phys. Rev. B **66**, 014414 (2002).

[13] M. V. Milosevic, S. V. Yampolskii, and F. M. Peeters, Phys. Rev. B **66**, 174519 (2002).

[14] D. J. Priour, Jr., and H. A. Fertig, Phys. Rev. Lett. **93**, 057003 (2004).

[15] M. V. Milosevic and F. M. Peeters, Phys. Rev. Lett. **93**, 267006 (2004).

[16] M. V. Milosevic and F. M. Peeters, Phys. Rev. Lett. **94**, 227001 (2005).

[17] M. M. Doria, A. R. de C. Romaguera, M. V. Milosevic, and F. M. Peeters, Europhys. Lett. **79**, 47006 (2007).

[18] M. Lange, M. J. Van Bael, Y. Bruynseraede, and V. V. Moshchalkov, Phys. Rev. Lett. **90**, 197006 (2003); M. Lange, M. J. Van Bael, A. V. Silhanek, and V. V. Moshchalkov Phys. Rev. B **72**, 052507 (2005).

[19] W. Gillijns, A. V. Silhanek, and V. V. Moshchalkov, Phys. Rev. B **74**, 220509(R) (2006).

[20] C. C. de Souza Silva, A. V. Silhanek, J. Van de Vondel, W. Gillijns, V. Metlushko, B. Ilic, and V. V. Moshchalkov, Phys. Rev. Lett. **98**, 117005 (2007).

[21] J. S. Neal, M. V. Milosevic, S. J. Bending, A. Potenza, L. San Emeterio, and C. H. Marrows, Phys. Rev. Lett. **99**, 127001 (2007).

[22] G. Carneiro, Phys. Rev. B **72**, 144514 (2005).

[23] J. R. Clem, in *Low Temperature Physics*, edited by K. D. Timmerhaus, W. J. O'Sullivan, and E. F. Hammel (Plenum, New York, 1974), Vol. 3, p. 102.

[24] P. Minnhagen, Rev. Mod. Phys. **59**, 1001 (1987).

[25] C. L. S. Lima, C. C. de Souza Silva, and G. Carneiro, private communication.

[26] A. V. Silhanek, L. Van Look, S. Raedts, R. Jonckheere, and V. V. Moshchalkov, Phys. Rev. B **68**, 214504 (2003).

[27] J. E. Villegas, E. M. Gonzalez, M. I. Montero, Ivan K. Schuller, and J. L. Vicent, Phys. Rev. B **68**, 224504 (2003).

[28] N. Verellen, A. V. Silhanek, W. Gillijns, V. V. Moshchalkov, V. Metlushko, F. Gozzini, and B. Ilic, Appl. Phys. Lett. **93**, 022507 (2008).